Mechanical Modeling of Low Temperature Superconducting Cables at the Strand Level

Pierre Manil, Miloud Mouzouri and François Nunio

***Abstract*— Low-temperature superconductors such as NbTi are widely used in high field magnets. The run for higher fields leads to greater forces on the conductor, which is pushed closer to its mechanical limit. Managing the higher stresses on the conductor supposes accurate mechanical models: it becomes necessary to simulate local peak stresses and strains, especially with Nb_3Sn conductors, which are mechanically brittle and strain-sensitive.**

Superconducting cables are anisotropic composite structures that can comprise superconducting strands, insulation materials and stabilizing parts.

This paper presents a convenient method for the geometrical modeling of composite superconducting Rutherford cables at the level of the strand. It is applied on the example of a cable-in-channel NbTi conductor. Our goal is to obtain a mesh of a cable sample that is suitable for Finite Elements (FE) Analysis, at the scale of the strand (around one millimeter), with a true-to-life contact configuration. Different methods and tools are discussed. Computed geometries are compared to tomographic data. Preliminary mechanical simulations with simplified parameters are done to verify the model convergence.

The ultimate goal of these explorations is to correlate the model results at the scale of the strand with experimental results at the scale of the cable, in order to identify the critical parameters that describe the best the conductor performance under mechanical solicitation.

***Index Terms*— Composite materials, hierarchical mechanical modeling, superconducting strands and cables, tomography.**

I. Introduction

SUPERCONDUCTING cables are anisotropic composite structures that can comprise twisted anisotropic superconducting strands, insulation materials and stabilizing parts. The compaction is rarely total and cavities can be present in the cable structure. Simulating local mechanical phenomena inside these structures becomes necessary because of the increasing magnetic fields and forces.

To reach higher fields, Nb_3Sn conductors are more and more used. But this intermetallic compound is brittle and strain-sensitive, and it shows performance degradation under mechanical solicitation [1]-[3]. As a consequence, local phenomena have a major impact on the large scale magnets behavior. Nowadays, the structural computations for magnets are mostly done at the scale of the cable (around one centimeter). They use homogenized material properties that account for all the cable components, using rules of mixture or experimental results. But in the future, magnet designers will need finer mechanical models of the superconductor down to the strand level (around one millimeter) and to the filament level (some tenths of a micron) [4]. The ultimate goal is to build an integrated hierarchical framework allowing correlation of large scale loads with local strains and stresses.

Numerous studies have been done in that direction [5]-[8], often focusing on a particular cable configuration. In [5], two-dimensional models are presented to get the filament strain state from the strand load. In [6], a hierarchical model of Nb_3Sn strands is presented, with a simplified contact representation. In [7], the strain states of numerous strands braided together in a cable-in-conduit are evaluated. The strands sections remain circular or elliptical. The closest study to our work has been led by Arbelaez and collaborators [8] and addresses many of the issues related to Rutherford cables hierarchical modeling, till the strand level. Initial cable geometry is carefully built, on the smallest possible unit cell. The full space is meshed, including surrounding air, with a fictitious void material. Deformed layout is obtained and compared to reality with nice correlation.

In this study, we also focus on the strand level. Void is not considered during the first calculation step, which consists in obtaining a true-to-life deformed strand geometry. Doing this, perfect contact is obtained between the strands after compression. The stresses are then reset and the other cable components (matrix, channel) are built with Computer-Aided Design (CAD) tools before mechanical analysis. The modeling down to the filament level is not treated.

For practical reasons, we have decided to work on the example of a cable-in-channel NbTi conductor designed for the MRI magnet Iseult. This cable is well known: tomographic and experimental data is available [9]. Moreover, its void fraction is close to zero due to a tin matrix, so it is reasonable to neglect the internal cavities as a first approximation. Our conclusions would remain the same with Nb_3Sn strands.

In the following, we describe the construction and validation of a relevant geometrical mesh of a 10 mm-long sample, for future FE computations.

Manuscript received 12 September 2011.

P. Manil and F. Nunio are with CEA Saclay/IRFU/SIS, 91191 Gif-sur-Yvette, France (phone: +33-1 69 08 74 79; e-mail: pierre.manil@cea.fr).

M. Mouzouri is with ENS Cachan, 61 avenue du Président Wilson, 94235 Cachan cedex, France.

II. Cable Geometry

A. Cable Features

The cable from Iseult main solenoid is represented in Fig. 1. It is a Rutherford cable-in-channel, with 9 NbTi/Cu strands embedded in a matrix of tin alloy. Its channel is made of copper. The main cable features are listed in Table I.

TABLE I. Cable Features

	Unit	Value
Number of strands	/	9
Strand diameter	mm	1.48
Twist pitch	mm	100
Cable width	mm	9.2
Cable thickness	mm	4.9

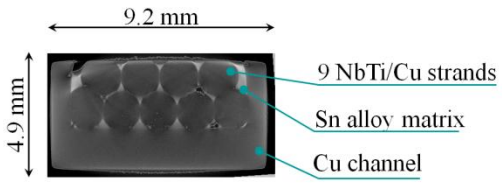

Fig. 1. Iseult cable cross-section.

B. X-Ray Tomography

A tomography has been performed on a 10 mm-long sample, with a 450 kV X-ray beam (Fig. 2). This is our reference geometry. The different components are visible, but their boundaries are not precise because of the poor contrast between components and the low transparence of the copper to the X-rays.

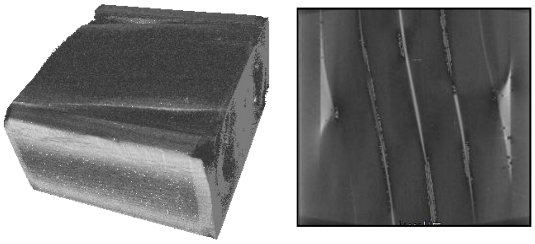

Fig. 2. RX tomography of an Iseult cable sample: isometric view (left); close-up from top (right).

C. Region Identification

As a first step, a region identification of the cable components is performed using a commercial code. The results are showed on Fig. 3. Due to the poor contrast, the identification is not clean at the boundaries, and many artifacts appear. This option is not satisfying for our purpose.

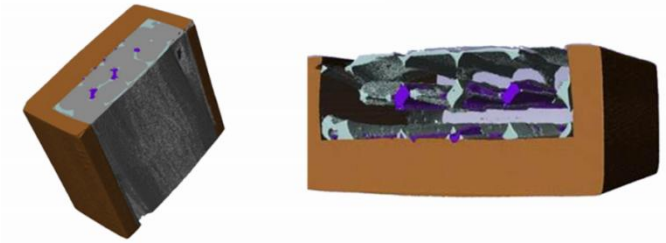

Fig. 3. Tomographic data post-treatment for material identification: whole sample (left); strands removed (right).

III. Geometrical Model of the Strands

Next option is to build 'by hand' the cable geometry. The main difficulty is to get the compressed strands shape. CAD tools would then easily generate the tin matrix and the channel.

A. Ideal Strands

A geometrical construction is done with CAD software using ideal strands, with a constant circular (or hexagonal) section (Fig. 4). The construction relies on several reference sections taken from the tomography. Separations and interpenetrations between strands are observed. We believe that they could be avoided with better 3D constraints, but such model would not be versatile enough to account for various cable layouts.

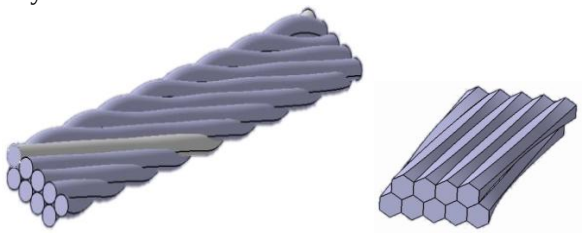

Fig. 4. Simplified CAD model of the strands with circular section (left) and hexagonal section (right).

B. Compressed Strands

A better option is to imitate the cable fabrication process. It is based on the FE method, using an explicit dynamic formulation. Even if the real process is slow, we benefit from the performances of fast dynamics codes. We don't prevent ourselves from playing with time-related parameters (for example the plates speed) when it improves the resulting geometry.

Two numerical tools are used: a preliminary model in ANSYS Autodyn [10] (with 9 000 nodes) and a full model in LS-DYNA [11] (with 400 000 nodes). The only goal of these computations is to get a realistic deformed shape. The mechanical results (stresses, strains) will not be considered, and the mesh will be converted into a solid part. Model simplifications are thus allowed. To limit computation times, we work on a 10 mm-long sample.

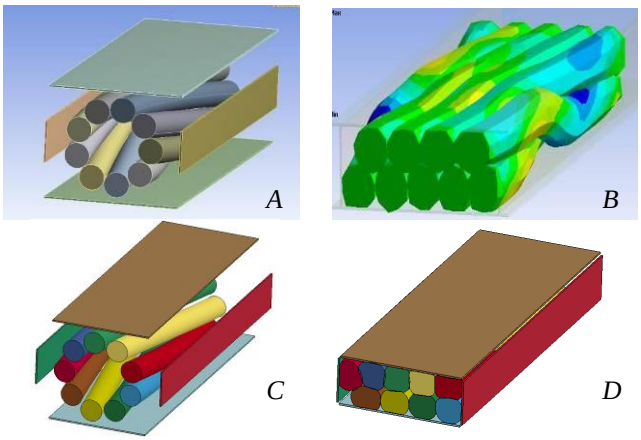

Fig. 5. Models of strands compression in ANSYS Autodyn (*A*, *B*) and in LS-DYNA (*C*, *D*).

The initial disposition of the cable is showed on Fig. 5.*A* and *C*. Initial strands have an ideal circular section of 1.48 mm. They are blocked longitudinally at the ends. They are oriented with a parameterized angle. Four rigid plates compress them with a parameterized speed till the target section size. After trying different sets of parameters with both codes, the deformed shapes represented in Fig. 5.*B* and *D* are obtained.

C. Geometrical Model Validation

Several sections are extracted from these results and compared to the tomographic data. A reference section (z=0 mm) is set when the cable 1 is at the lower left-hand corner (Fig. 6). At a first glance, the models are in good agreement with reality all over the sample.

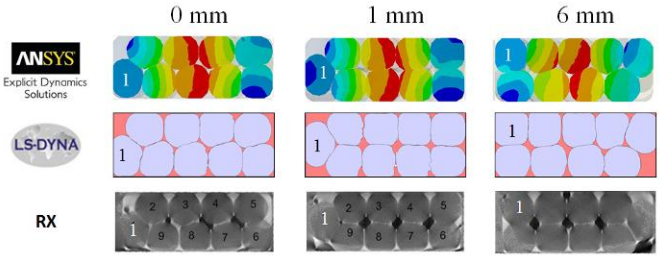

Fig. 6. Cross-sections of the compressed strands calculated in ANSYS Autodyn and LS-DYNA, compared geometrically with the tomographic data. The reference section (z=0 mm) has been chosen arbitrarily. Two additional sections are compared (z=1 mm and z=6 mm).

The proposed criterion for a quantified comparison is the contact zone length between the components (strands and channel). For each section, a symmetric matrix containing this data is build and compared to the tomographic data. The average discrepancy is of the order of 5 to 10 %. This is not negligible, but we believe it is realistic enough for preliminary mechanical modeling. The results could be easily improved and adjusted by playing with the parameters.

IV. Mechanical Model of the Sample

A. Geometrical Model of the Sample

The mesh from LS-DYNA is fitted strand by strand before importation in our CAD software. An important cleaning of the geometry is necessary: local artifacts created during fitting must be removed. The boundaries of the cables are reshaped to match a perfect rectangular section. This time-consuming defeaturing task cannot easily be automated.

The tin matrix is obtained by Boolean operation. It has three separate parts. Some erratic volumes (with very small thickness or volume) are suppressed by hand. The copper channel is designed numerically with an ideal shape. The whole space is filled: our model doesn't account for internal cavities. CAD geometries are represented in Fig. 7.

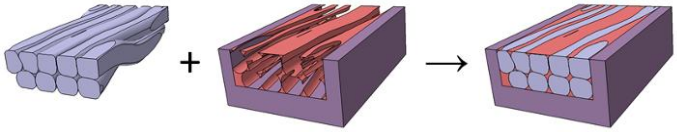

Fig. 7. CAD construction of the cable sample model. The compressed strands (left) resulting from a dynamic computation in LS-DYNA are imported. The tin matrix and copper channel (center) are designed using CAD tools.

B. Meshing

The sample geometry is imported in ANSYS Workbench. To gain time, the default auto-meshing parameters are set: fine relevance center, default element size, medium smoothing, fast transition, medium span angle center, smooth transition inflation. Triangular elements are used in the strands and in the matrix, whereas parallelepipeds are used for the channel. Both of them use quadratic formulation. These choices, controlled by the meshing tool, ensure rather fast and efficient meshing. The density of triangular elements in the strands is sufficient to meet our objectives.

A mesh with 250 000 nodes is generated successfully (Fig. 8). A significant proportion of elements have a distorted shape, especially in the matrix. Up to now, the mesh is non-conformal, but in the future we would rather have matching nodes at the interfaces.

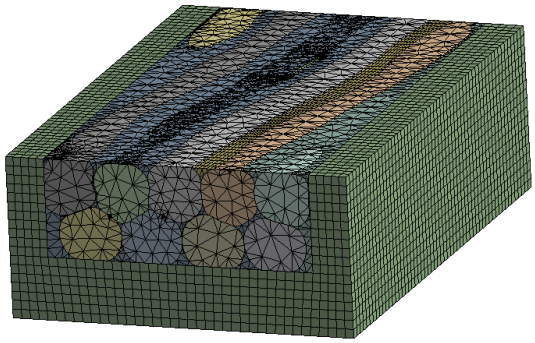

Fig. 8. Mesh of the cable sample (250 000 nodes).

C. Mechanical Model

The sample mesh includes complex contacts, particularly around the strands. The distorted elements generated around these boundaries could prevent numerical convergence or alter the results. A thorough verification must be done.

In this purpose and as a first check, the contacts are glued and the whole materials are set to steel with a Young modulus equal to 200 GPa and a Poisson's coefficient equal to 0.3. Simple load cases are calculated, involving compression, traction and/or shear. Fig. 9 illustrates three test cases: compressive load of 50 MPa on the labeled top surface (*A*), traction of 50 MPa on the labeled lateral surface (*B*), tangent force on the top surface (*C*). The usual boundary conditions are set accordingly. The computed displacement is extracted at one probe node, located at the center of the solicited surface. The probe displacement is compared to the one of a witness model involving a parallelepiped block of the same dimensions, with the same materiel properties. The results are compared in Table II.

The agreement is very satisfying. The model can be used further. Let's point that the discrepancy is lower when the longitudinal contact zones are less solicited (case *A*).

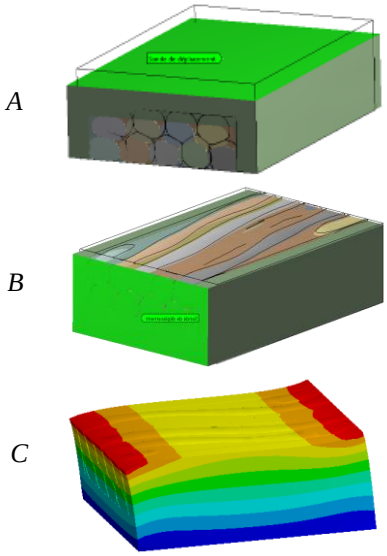

Fig. 9. Mechanical model validation using the material properties of steel everywhere and glued contacts, for comparison with a plain steel block (ANSYS). Deformations are amplified.

TABLE II. NUMERICAL TEST RESULTS

Load Case	Probe Displacement (μm)		
	Steel Block	Steel on Cable Mesh	Difference (%)
Case *A*	1.05	1.06	0.1
Case *B*	3.25	3.29	1.2
Case *C*	4.49	4.39	2.2

D. Computation trials

We would like to increase gradually the model complexity to approach reality. This process is on-going, and only preliminary results are shown.

At first, plasticity is neglected: elastic copper is assigned to the strands and channel, elastic tin is assigned to the matrix. The contacts are glued. Doing this, our model is totally linear. A compressive load (homogeneous pressure) is applied to the bottom surface of the channel. The opposite surface is blocked in the normal direction.

The computation converges. The resulting stresses are represented in Fig. 10, at the scale of the strand, for a pressure of 50 MPa. These values are for illustration and have no mechanical meaning at the moment.

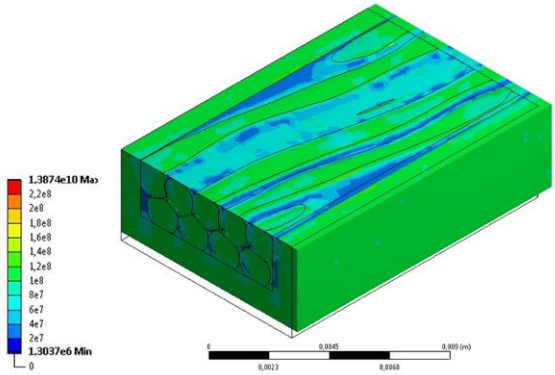

Fig. 10. Von Mises stresses (Pa) on the sample under compression (50 MPa).

V. DISCUSSION

This study has led to mesh successfully conductor samples at the scale of a strand. The modeled strand deformations and contact zones are true-to-life and in perfect contact.

First mechanical calculations with elastic material properties confirm that our model can converge. But it is far too early to use these results for practical applications. Many improvements are necessary. Implementing plasticity will lead to a non-linear model, increasing considerably the computation times. Allowing contact separation with friction or sliding will also increase the model complexity. This will be necessary when the cavities will be represented. At end, the superconducting strand properties are not isotropic, and the local coordinate system is not standard. Also, even if this study gives very encouraging results in terms of geometrical construction and model convergence, a considerable work is necessary to get a reliable conception tool.

ACKNOWLEDGMENT

The authors would like to thank Christophe Berriaud, Thibault Lécrevisse, Etienne Rochepault and Pierre Védrine for the input data.

REFERENCES

[1] T. Kate, et al., "The reduction of the critical current in Nb_3Sn cables under transverse forces", *IEEE Trans. Applied Superconductivity*, vol. 28, Issue 1, pp. 715 - 718, 1992

[2] M.C. Jewell, "The effect of strands architecture on the fracture propensity of Nb_3Sn composite wires", PhD thesis for the University of Wisconsin, Madison, 2008

[3] A. Nijhuis, Y. Ilyin, W. Wessel, "Spatial periodic contact stress and critical current of a Nb_3Sn strand measured in TARSIS", *Supercond Sci. Technol.*, vol. 19, pp. 1089-1096, 2006

[4] P. Ferracin, "Modeling techniques for design and analysis of superconducting accelerator magnets", ICAP09, San Francisco, 2009.

[5] N. Mitchell, "Modeling of the effect of Nb_3Sn strand composition on thermal strains and superconducting performance", *IEEE Trans. Applied Superconductivity*, vol. 15, Issue 2, pp. 3572 - 3576, 2005

[6] D.P. Boso, M. Lefik and B.A. Schrefler, "A multilevel homogenised model for superconducting strand thermomechanics", *Cryogenics*, vol. 45, Issue 4, pp. 259-271, 2004.

[7] H. Bajas, D. Durville, D. Ciazynski, A. Devred, "Numerical Simulation of the Mechanical Behaviour of ITER Cable-in-conduit Conductors", *IEEE Trans. Applied Superconductivity*, vol. 20, Issue 3, pp. 1467 - 1470, 2010

[8] D. Arbelaez, S.O. Prestemon, P. Ferracin, A. Godeke, D.R. Dietderich, G. Sabbi, "Cable deformation simulation and a hierarchical framework for Nb_3Sn Rutherford cables", *J. Phys.: Conf. Ser.*, vol. 234, Part 2, 2010

[9] C. Berriaud, *et al.*, "Iseult/INUMAC 11.7 T MRI Magnet Conductor Production Status", submitted to these proceedings.

[10] www.ansys.com/Products/Simulation+Technology/Explicit+Dynamics/Features

[11] www.ls-dyna.com